Publication Year	2024
Acceptance in OA	2026-01-14T13:22:51Z
Title	Euclid preparation: LI. Forecasting the recovery of galaxy physical properties and their relations with template-fitting and machine-learning methods
Authors	Euclid Collaboration, Enia, A., BOLZONELLA, Micol, POZZETTI, Lucia, Humphrey, A., Cunha, P. A. C., Hartley, W. G., Dubath, F., Paltani, S., Lopez Lopez, X., Quai, S., BARDELLI, Sandro, BISIGELLO, Laura, CAVUOTI, STEFANO, DE LUCIA, GABRIELLA, Ginolfi, M., GRAZIAN, Andrea, Siudek, M., TORTORA, CRESCENZO, Zamorani, G., Aghanim, N., Altieri, B., Amara, A., ANDREON, Stefano, AURICCHIO, NATALIA, Baccigalupi, C., Baldi, M., Bender, R., Bodendorf, C., BONINO, Donata, Branchini, Enzo, BRESCIA, Massimo, Brinchmann, J., Camera, S., Capobianco, Vito, CARBONE, Carmelita, Carretero, J., Casas, S., Castander, F. J., CASTELLANO, Marco, Castignani, G., Cimatti, A., Colodro-Conde, C., Congedo, G., Conselice, C. J., Conversi, L., Copin, Y., CORCIONE, Leonardo, Courbin, F., Courtois, H. M., Da Silva, A., Degaudenzi, H., DI GIORGIO, Anna Maria, Dinis, J., Dupac, X., Dusini, S., Fabricius, M., FARINA, Maria, Farrens, S., Ferriol, S., Fosalba, P., Fotopoulou, S., FRAILIS, Marco, FRANCESCHI, ENRICO, FUMANA, Marco, GALEOTTA, Samuele, Gillis, B., GIOCOLI, Carlo, Grupp, F., Haugan, S. V. H., Holmes, W., Hook, I., Hormuth, F., Hornstrup, A., Jahnke, K., Joachimi, B., Keihänen, E., Kermiche, S., Kiessling, A., Kubik, B., Kümmel, M., Kunz, M., Kurki-Suonio, H., LIGORI, Sebastiano, Lilje, P. B., Lindholm, V., Lloro, I., MAIORANO, Elisabetta, MANSUTTI, Oriana, Marggraf, O., Markovic, K., Martinelli, M., Martinet, N., Marulli, F., Massey, R., McCracken, H. J., Medinaceli, E., Mei, S., Melchior, M., Mellier, Y., MENEGHETTI, MASSIMO, MERLIN, Emiliano, Meylan, G., Moresco, M., Moscardini, L., MUNARI, Emiliano, Neissner, C., Niemi, S. -M., Nightingale, J. W., Padilla, C., Pasian, F., Pedersen, K., Pettorino, V., Polenta, G., Poncet, M., Popa, L. A., Raison, F., Rebolo, R., Renzi, A., Rhodes, J., RICCIO, GIUSEPPE, ROMELLI, Erik, Roncarelli, M., Rossetti, E., Saglia, R., Sakr, Z., Sapone, D., Schneider, P., Schrabback, T., SCODEGGIO, MARCO, Secroun, A., SEFUSATTI, Emiliano, Seidel, G., Serrano, S., Sirignano, C., Sirri, G., Stanco, L., Steinwagner, J., Surace, C., Tallada-Crespí, P., TAVAGNACCO, Daniele, Taylor, A. N., Teplitz, H. I., Tereno, I., Toledo-Moreo, R., Torradeflot, F., Tutusaus, I., VALENZIANO, Luca, Vassallo, T., Verdoes Kleijn, G., Veropalumbo, A., Wang, Y., Weller, J., ZUCCA, Elena, BIVIANO, ANDREA, Boucaud, A., BURIGANA, Carlo, Calabrese, M., Escartin Vigo, J. A., Gracia-Carpio, J., Mauri, N., Pezzotta, A., Pöntinen, M., Porciani, C., Scottez, V., Tenti, M., VIEL, Matteo, Wiesmann, M., Akrami, Y., Allevato, V., Anselmi, S., Ballardini, M., Bergamini, P., Bethermin, M., Blanchard, A., Blot, L., BORGANI, Stefano, Bruton, S., Cabanac, R., Calabro, A., Canas-Herrera, G., CAPPI, Alberto, Carvalho, C. S., Castro, T., Chambers, K. C., Contarini, S., Contini, T., Cooray, A. R., CUCCIATI, Olga, Davini, S., De Caro, B., Desprez, G., Díaz-Sánchez, A., Di Domizio, S., Dole, H., Escoffier,

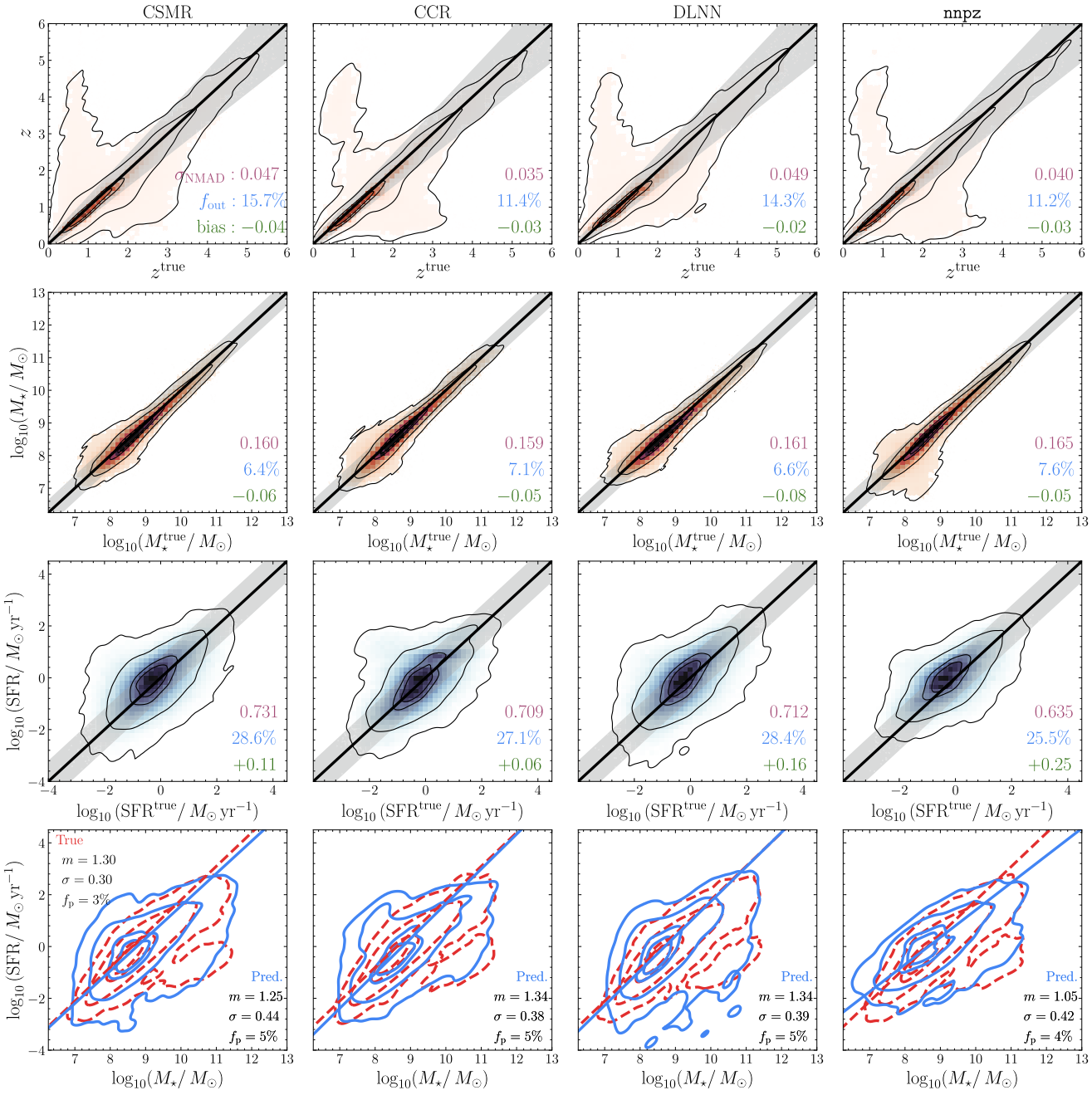

Fig. 10. Results for the EDF. Each column represents the results for the methods described in Sect. 3. The first three rows are the labels, with the true value plotted against the predicted one. The fourth column is the MSFS, with true values in red (dashed) and predicted ones in blue (solid). The reported metrics are the NMAD (purple), outlier fraction $f_{\rm out}$ (blue), the bias (green), and for the SFMS the slope (α), the scatter (σ) and fraction of passive galaxies ($f_{\rm p}$), all defined in Sect. 3.6.

informative wavelengths out of the region sampled by *Euclid*. As such, those will hamper the naturally expected metrics improvement for Wide-alike sources observed at Deep uncertainty level. For the sake of comparison, in Table 7 we also report the corresponding metrics obtained by applying the same photometric cuts from the EWS to the EDF test galaxies (see Sect. 2 for further details).

The results are reported in Fig. 10. It is immediately visible how the EDF goes farther in distance (contours extending significantly at $z > 4$) and at lower masses and SFRs. The photo-zs NMAD values are comparable, though lower (0.04–0.05) than the best ones reached for the EWS (0.05–0.06). The same is true for outliers, with a reduction of 1%–3% despite the presence of a cloud of low-z galaxies spread over $1.5 < z_{\rm phot} < 5$. Those are fainter, low-mass galaxies with $\log_{10}(M_\star/M_\odot) < 8$ which were marginally detected in the EWS but are one order of magnitude more present in the EDF. If we apply the Wide cuts to the Deep test galaxies, we observe a dramatic improvement in the metrics, as the NMAD for photo-z falls to ∼0.02–0.04 with only ∼1% of outliers for both `nnpz` and CCR.

A significant improvement is observed also for the stellar masses, even without parceling out the fainter galaxies from the Wide-alike, as for the photo-z. This is principally a consequence of the addition of the two IRAC filters and, secondly, of the

Table 7. Metrics for the EDF, with the same EWS photometric cuts to the test galaxies.

	CSMR			CCR			DLNN			nnpz		
	NMAD	f_{out}	bias	NMAD	f_{out}	bias	NMAD	f_{out}	bias	NMAD	f_{out}	bias
z	0.02	1.8%	−0.03	0.02	0.9%	−0.03	0.03	3.2%	0.00	0.02	0.9%	−0.02
$M_\star$	0.12	2.5%	−0.10	0.12	2.5%	−0.09	0.12	4.7%	0.01	0.13	2.2%	−0.06
SFR	0.60	23.4%	0.13	0.61	22.1%	0.13	0.63	25.4%	0.22	0.63	22.5%	0.13

Notes. $M_\star$ refers to $\log_{10}(M_\star/M_\odot)$, SFR to $\log_{10}(\mathrm{SFR}/M_\odot\,\mathrm{yr}^{-1})$.

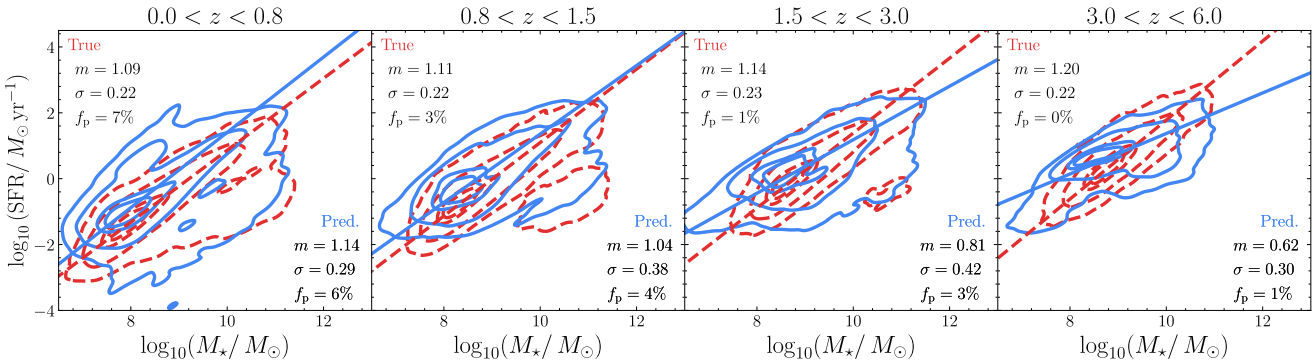

Fig. 11. Results for the recovered SFMS in the EDF, in four different redshift bins. Test values are in red (dashed) and predicted ones in blue (solid). The reported metrics are defined in Sect. 3.6.

improved photometry. All the codes show a net improvement for NMADs, outlier fractions, and biases, even for the full set of test galaxies (down to NMADs of ∼0.16 and $f_{out} \sim 13\%$. If accounting only for the Wide cut, the net improvement gets important, falling to NMAD ∼ 0.12 and $f_{out} \sim 2.5\%$.

SFRs show a different behavior for the full set of test data. This is due to a particular set of outliers, low star-forming galaxies [$\log_{10}(\mathrm{SFR}/M_\odot\,\mathrm{yr}^{-1}) < -1$] that are mistakenly predicted as higher $\log_{10}(\mathrm{SFR}/M_\odot\,\mathrm{yr}^{-1}) > 0$ due to a wrong photo-z attribution that impacts the SFRs, visible as the strip of $z^{\mathrm{true}} \sim 1$ galaxies in the top panels of Fig. 10. When applying the EWS photometric cuts, the NMADs are lower than those found in the mixed labels Deep – Wide case. The same applies for f_{out} and the bias.

There is a notable exception, as nnpz is able to reduce the impact of these outliers, to the point where even the full set of test data gives back comparable results to the mixed labels Deep – Wide case and better for the EWS-cut ones. This is both a consequence of a better photo-z estimation and an overall better ability of nnpz in recovering the SFRs given the input set of features, as also observed in Sect. 4.4.

Overall, the MS recovery is optimal in the EDF. Of all the considered methods, CCR and nnpz are the ones returning the best overall results, as the former optimally recovers photo-zs and stellar masses, while the latter recovers the SFRs the best. If we perform a binning in redshift, we observe how the best results are obtained when the stellar masses and SFRs are optimally recovered (as the true redshift is) – thus at $0.8 < z < 1.5$ – and worse ones at higher-z, where lots of low-z objects are mistakenly placed at high-z with greatly enhanced stellar masses (and to a lesser extent the SFRs), thus bending the whole relation by a significant amount (see rightmost plot in Fig. 11). At lower-z, we notice a symmetric issue, with lots of low-mass and $\log_{10}(\mathrm{SFR}/M_\odot\,\mathrm{yr}^{-1}) \sim 0$ galaxies removed from the binning as the models place those at $z > 2$, and thus the predicted relation differs significantly from the true one.

There are reasons for optimism. First of all, we stress that these results should be considered lower-limit performance. Forty ROS are the minimum number expected for the EDF, with the highest going up to 53. We expect that increasing the number of ROS will produce better performance, at least slightly (the order of a few percentage points), even though it is not straightforward to assess as mentioned before. In fact, the improvement in metrics seems to saturate after a certain number of ROS. We can roughly quantify, by extrapolating from the different realizations of the metrics for the four different number of ROS used in this work, a reduction of a few percentage points in NMAD and f_{out} with 53 ROS, both with template-fitting and ML methods.

All those results are limited to the UNIONS+*Euclid*+two IRAC filters, which do not extend over the 4.5 µm observed-frame, with a gap between the H_E band and IRAC. The more the galaxies move to higher redshift, the more these particular sets of features will probe the source UV-rest frame, which is less sensible to stellar masses and more to SFRs. However, the EDF, given their extension and importance in galaxy formation and evolution, will benefit from a wealth of ancillary and upcoming multiwavelength data from UV to radio. For example, the EDF-South has been observed with the MeerKAT program MKT-23041 (P.I. Prandoni); the EDF-N is currently proposed to be observed with the LOFAR2.0 Ultra-Deep Observation (LUDO), whose 2 µJy beam^{-1} at 150 MHz would translate into one of the deepest radio observations ever, and it has already been observed at 144 MHz with a central rms of 32 µJy beam^{-1} (Bondi et al. 2024); as illustrated, all the EDF has been covered with *Spitzer* at 3.6 and 4.5 µm (Euclid Collaboration 2022a); deep observations in U band with CFHT (Euclid Collaboration 2024i) are currently ongoing; the same for deep optical observations with Hyper Suprime Cam (Euclid Collaboration 2024e); K band observations with VISTA of the EDF-S have been taken as part of the EDFS-Ks program, down to a limiting magnitude of 23.5 (PI Nonino), covering the gap between the H_E band and IRAC. Extending the feature space with mid-IR to submillimeter

and radio fluxes will undoubtedly produce better, more reliable physical parameters than those reported in this work.

5. Summary

Euclid and the forthcoming large-scale surveys – *Rubin*/LSST, *Roman*) – will benefit from unprecedentedly sampled areas of the sky, with an estimated number of observed sources up to the order of billions. At those scales, automated, accurate, and rapid methods to assess photometric redshifts and physical properties from the observables must be developed and tested.

In this study, we evaluated the performance of `Phosphoros`, a template-fitting algorithm, with four ML methods for the recovery of photo-zs, stellar masses, star formation rates, and the SFMS: two `CatBoost`-based methods roote GBDT, a single-pass regressor (CSMR) and a chained regressor ensemble (CCR); a simple and plain DLNN; and `nnpz`, an enhanced nearest-neighbors algorithm capable of handling the full parameter posteriors. As it is typical in ML applications, the quality of the recovered labels is inevitably limited by the number and quality of input information entering the model. Noisy features hamper a plain association between those and the labels, degrading the final performance.

In order to realistically quantify how reliable *Euclid* photo-zs and physical parameters will be, we simulated observations of both the EWS and the EDF with ground-based *ugriz* and *Euclid* filters (plus two IRAC channels for the latter). The simulations are obtained within the MAMBO workflow, an empirical method to extract galaxies' physical information from simulated light-cones. We also simulated an intermediate number of ROS mimicking what is expected from the *Euclid* auxiliary fields, observations of well-known fields in the sky where a wealth of ancillary multiwavelength data is available for optimal photometric and color calibration. Finally, we run all the methods on an unperturbed version of the mocks, that is, without any photometric noise added and trained on the labels true values, serving as an unrealistic best-case scenario for the performance given that particular set of features (magnitudes and pairwise differences, the colors).

We found how, in the unperturbed catalog, that set of 45 features is more than enough for the models to almost perfectly recover photometric redshifts and stellar masses (NMAD $<$ 0.03, $f_{\rm out}$ $<$ 0.3%). Things are more complicated for star formation rates, with NMADs never falling below 0.16. This is expected, as the SFR correlates weakly with the input labels that sample the 0.3–1.8 µm observed-frame wavelength range but correlates strongly with the 8–1000 µm integrated luminosity (and monochromatic flux in the UV at 2800 Å rest-frame).

When feeding the mock photometry to `Phosphoros` either for the EWS or the EDF, we observe a typical pattern where the vast majority of outliers are generated by low-z galaxies (z $<$ 1) misplaced at $1.5 < z < 5$, with predicted higher values of $\log_{10}(M_\star/M_\odot) > 10$ instead of ∼8.5, and $\log_{10}(\mathrm{SFR}/M_\odot\,\mathrm{yr}^{-1}) > 0.5$ instead of $-2 < \log_{10}(\mathrm{SFR}/M_\odot\,\mathrm{yr}^{-1}) < -1$. The SFMS is poorly recovered in the EWS, while better though suboptimal results are observed for the EDF, suggesting the need for better-suited, ad hoc priors to adopt for template-fitting.

As we want to evaluate the ML methods with what *Euclid* will realistically yield, their EWS and EDF performance are measured training on `Phosphoros` recovered labels and testing on true values. We also checked the metrics improvement when training on true values – inaccessible in a real scenario, as the ground truth is unknown. Moreover, since we simulated four different versions of the mock catalogs (EWS, EDF, and two auxilliary fields named C16 and C25 from the number of expected ROS), for the EWS we test how a model trained on features and labels coming from deeper photometry fare on the test EWS ground truth values.

We found different results by employing two approaches: in the paired labels approach, we are training the models on a rightly coupled set of features and labels coming respectively from the four catalogs and testing on the EWS ground truth. With this approach, we notice a well-known pattern in ML applications: as there is a mismatch between the training and test features (in terms of noise), it is not guaranteed that a deeper set of features (and labels) would lead to better performance. This is particularly true for stellar masses, as the NMADs and fraction of outliers do not improve significantly (or become even worse, see Table C.1) from training and testing on the EWS to training on deeper photometries and testing on the EWS, with the notable exception of EDF training as it benefits from the addition of two IRAC filters.

Better performance is obtained if we employ a mixed labels approach. In this case, the labels are still the `Phosphoros` results on photometry coming from the four catalogs, but the training features are always the ones from the EWS. Despite the reduction in the training sample size (as only EWS detected sources are employed in training) from a few million to ∼500 k sources, this approach avoids the data mismatch issue, as the features always come from the EWS simulated catalog. More importantly, it acts as a prior on the features-labels association, as the models are able to better distinguish between similar cases near degenerate regions of the feature space, for instance, the ones that generate the outlier cloud of close and less massive galaxies mistaken for far-away and more massive ones.

In fact, those outliers are significantly reduced (or disappear altogether) with this approach. We observed a significant improvement in the performance metrics, matching or even surpassing those obtained with `Phosphoros`: for `nnpz`, $z_{\rm phot}$ NMAD decreases from 0.063 to 0.055, and $f_{\rm out}$ is reduced from 22% to 15% passing from Wide training labels to Deep training labels, not so distant from the ideal scenario when the true labels are known (0.047 and 15% respectively). The same goes for stellar masses (for the CCR, NMAD falls from 0.24 to 0.19, outliers from 28% to 11%, while they are 0.14 and 10% in the ideal scenario) and star formation rates (`nnpz` reaches NMADs of 0.62 starting from 0.71, and outliers of 23% from 30%, lower limits of 0.43 and 11%). The same is true for the MS.

The full EDF would not be finalized until February 2031. In the meantime, the main scientific results will rely on training samples obtained from multiple ROS of the auxiliary fields. We observed how the metrics did not degrade by more than a few percentage points between the C16 and C25 training samples (though here we only use the 9 previously cited bands to infer the results, thus the real ones will benefit from better estimated labels) and the EDF one. Moreover, we also checked how a COSMOS-like reference sample does not significantly impact the model performance, as a reduction to ∼230 k galaxies in the training sample is not enough to degrade those by more than 1–2%. As a final test, we removed the *u* band filter from the test sample, as we already know that, for DR1, those observations of the southern sky will not yet be available. However, that should not compromise the scientific outcome, as we only notice a small performance degradation, on the order of ∼3%.

As expected, the EDF results are the ones with the best results, where both labels and features come from the deepest available observations (and `Phosphoros` run on). The parameter recovery is optimal, especially the MS, once considered how

the EDF extends the object detection to significantly higher redshifts (one order of magnitude more $z > 4$ galaxies) and lower stellar masses and SFRs, with one order of magnitude increase for $\log_{10}(M_\star/M_\odot) < 8$ and $\log_{10}(\mathrm{SFR}/M_\odot\,\mathrm{yr}^{-1}) < 0$.

There are some caveats to keep in mind to properly gauge all those results in the right framework. In our simulated catalogs, we are only considering galaxies, thus neglecting the potential impact of misclassified stars, AGN and QSOs, local contaminants, and photometric defects. These will undoubtedly cause a degradation in the considered metrics, at least by a few percent, even though a precise quantitative estimation is nontrivial and outside the scope of this work. The simulated EWS and EDF are built assuming BC03 models; thus, whatever discrepancy might come from what an actual galaxy emission is (or the chosen IMF) will impact the overall performance, again, in a nontrivial way. Also, we are evaluating performance on the EWS and EDF simulated catalogs with nine filters, the ground-based *ugriz* and four *Euclid* ones. This is the bare minimum that will be released by *Euclid*, but we know that, especially for the ∼53 deg^2 of the EDF given their importance in the galaxy formation and evolution context, multiple ancillary or forthcoming multiwavelength data will be available to complement the *Euclid* releases.

As such, we can consider our results as a kind of best-case – as we are not accounting for defects in the catalog, the contamination by AGNs, and the fact that galaxy emission could differ from BC03 models – of the worst-case scenario, as adding more filters, especially in the mid-IR to far-IR, will undeniably improve the performance. These results highlight *Euclid*'s vast potential in assessing galaxy formation and evolution and could serve as a benchmark for all the upcoming large-area surveys in the next decade.

Acknowledgements. The Euclid Consortium acknowledges the European Space Agency and a number of agencies and institutes that have supported the development of *Euclid*, in particular the Agenzia Spaziale Italiana, the Austrian Forschungsförderungsgesellschaft funded through BMK, the Belgian Science Policy, the Canadian Euclid Consortium, the Deutsches Zentrum für Luft- und Raumfahrt, the DTU Space and the Niels Bohr Institute in Denmark, the French Centre National d'Etudes Spatiales, the Fundação para a Ciência e a Tecnologia, the Hungarian Academy of Sciences, the Ministerio de Ciencia, Innovación y Universidades, the National Aeronautics and Space Administration, the National Astronomical Observatory of Japan, the Netherlandse Onderzoekschool Voor Astronomie, the Norwegian Space Agency, the Research Council of Finland, the Romanian Space Agency, the State Secretariat for Education, Research, and Innovation (SERI) at the Swiss Space Office (SSO), and the United Kingdom Space Agency. A complete and detailed list is available on the *Euclid* web site (www.euclid-ec.org). AE, MB, LP, SQ, MT, GDL, VA, JB, SF, MS acknowledge support from the ELSA project. "ELSA: Euclid Legacy Science Advanced analysis tools" (Grant Agreement no. 101135203) is funded by the European Union. Views and opinions expressed are however those of the author(s) only and do not necessarily reflect those of the European Union or Innovate UK. Neither the European Union nor the granting authority can be held responsible for them. UK participation is funded through the UK HORIZON guarantee scheme under Innovate UK grant 10093177. We acknowledge the support from grant PRIN MIUR 2017-20173ML3WW_s. We acknowledge the CINECA award under the ISCRA initiative, for the availability of high performance computing resources and support. M.S. acknowledges support by the Polish National Agency for Academic Exchange (Bekker grant BPN/BEK/2021/1/00298/DEC/1), the State Research Agency of the Spanish Ministry of Science and Innovation under the grants 'Galaxy Evolution with Artificial Intelligence' (PGC2018-100852-A-I00) and 'BASALT' (PID2021-126838NB-I00). This work was partially supported by the European Union's Horizon 2020 Research and Innovation program under the Maria Sklodowska-Curie grant agreement (No. 754510). `Phosphoros` filters are taken from the SVO Filter Profile Service (Rodrigo et al. 2012; Rodrigo & Solano 2020). This research has made use of the Spanish Virtual Observatory (https://svo.cab.inta-csic.es) project funded by MCIN/AEI/10.13039/501100011033/ through grant PID2020-112949GB-I00. In preparation for this work, we used the following codes for Python: `Numpy` (Harris et al. 2020), `Scipy` (Virtanen et al. 2020), `Scikit-Learn` (Pedregosa 2011), `Pandas` (Wes McKinney 2010), `CatBoost` (Prokhorenkova et al. 2018), `Tensorflow` (Abadi et al. 2016), `nnpz` (Tanaka et al. 2018), `Phosphoros` (Paltani et al., in prep.).

References

Abadi, M., Agarwal, A., Barham, P., et al. 2016, arXiv e-prints [arXiv:1603.04467]
Akeson, R., Armus, L., Bachelet, E., et al. 2019, arXiv e-prints [arXiv:1902.05569]
Alsing, J., Peiris, H., Mortlock, D., Leja, J., & Leistedt, B. 2023, ApJS, 264, 29
Alsing, J., Thorp, S., Deger, S., et al. 2024, ApJS, 274, 12
Angulo, R. E., & White, S. D. M. 2010, MNRAS, 405, 143
Bell, E. F., & Kennicutt, R. C., Jr. 2001, ApJ, 548, 681
Bell, E. F., Papovich, C., Wolf, C., et al. 2005, ApJ, 625, 23
Bondi, M., Scaramella, R., Zamorani, G., et al. 2024, A&A, 683, A179
Bonjean, V., Aghanim, N., Salomé, P., et al. 2019, A&A, 622, A137
Bowles, M., Scaife, A. M. M., Porter, F., Tang, H., & Bastien, D. J. 2021, MNRAS, 501, 4579
Brescia, M., Cavuoti, S., D'Abrusco, R., Longo, G., & Mercurio, A. 2013, ApJ, 772, 140
Bruzual, G., & Charlot, S. 2003, MNRAS, 344, 1000
Calzetti, D., Armus, L., Bohlin, R. C., et al. 2000, ApJ, 533, 682
Carvajal, R., Matute, I., Afonso, J., et al. 2023, A&A, 679, A101
Cavuoti, S., Tortora, C., Brescia, M., et al. 2017, MNRAS, 466, 2039
Chabrier, G. 2003, PASP, 115, 763
Chambers, K. C., Magnier, E. A., Metcalfe, N., et al. 2016, arXiv e-prints [arXiv:1612.05560]
Collister, A. A., & Lahav, O. 2004, PASP, 116, 345
Cropper, M., Pottinger, S., Niemi, S., et al. 2016, SPIE Conf. Ser., 9904, 99040Q
Cunha, P. A. C., & Humphrey, A. 2022, A&A, 666, A87
Daddi, E., Dickinson, M., Morrison, G., et al. 2007, ApJ, 670, 156
Dark Energy Survey Collaboration (Abbott, T., et al.) 2016, MNRAS, 460, 1270
Davidzon, I., Jegatheesan, K., Ilbert, O., et al. 2022, A&A, 665, A34
Delli Veneri, M., Cavuoti, S., Brescia, M., Longo, G., & Riccio, G. 2019, MNRAS, 486, 1377
Dieleman, S., Willett, K. W., & Dambre, J. 2015, MNRAS, 450, 1441
D'Isanto, A., & Polsterer, K. L. 2018, A&A, 609, A111
Euclid Collaboration (Desprez, G., et al.) 2020, A&A, 644, A31
Euclid Collaboration (Moneti, A., et al.) 2022a, A&A, 658, A126
Euclid Collaboration (Schirmer, M., et al.) 2022b, A&A, 662, A92
Euclid Collaboration (Bisigello, L., et al.) 2023, MNRAS, 520, 3529
Euclid Collaboration (Aussel, B., et al.) 2024a, A&A, 689, A274
Euclid Collaboration (Cropper, M., et al.) 2024b, A&A, in press https://doi.org/10.1051/0004-6361/202450996
Euclid Collaboration (Jahnke, K., et al.) 2024c, A&A, in press https://doi.org/10.1051/0004-6361/202450786
Euclid Collaboration (Leuzzi, L., et al.) 2024d, A&A, 681, A68
Euclid Collaboration (McPartland, C. J. R., et al.) 2024e, A&A, submitted [arXiv:2408.05275]
Euclid Collaboration (Mellier, Y., et al.) 2024f, A&A, in press https://doi.org/10.1051/0004-6361/202450810
Euclid Collaboration (Paltani, S., et al.) 2024g, A&A, 681, A66
Euclid Collaboration (Scaramella, R., et al.) 2024h, A&A, 662, A112
Euclid Collaboration (Zalesky, L., et al.) 2024i, A&A, submitted [arXiv:2408.05296]
Fazio, G. G., Hora, J. L., Allen, L. E., et al. 2004, ApJS, 154, 10
Firth, A. E., Lahav, O., & Somerville, R. S. 2003, MNRAS, 339, 1195
Flaugher, B., Diehl, H. T., Honscheid, K., et al. 2015, AJ, 150, 150
Galametz, A., Saglia, R., Paltani, S., Apostolakos, N., & Dubath, P. 2017, A&A, 598, A20
Gentile, F., Tortora, C., Covone, G., et al. 2022, MNRAS, 510, 500
Gentile, F., Tortora, C., Covone, G., et al. 2023, MNRAS, 522, 5442
Girelli, G. 2021, Ph.D. Thesis, Alma Mater Studiorum Università, Italy
Girelli, G., Bolzonella, M., & Cimatti, A. 2019, A&A, 632, A80
Girelli, G., Pozzetti, L., Bolzonella, M., et al. 2020, A&A, 634, A135
Grazian, A., Fontana, A., Santini, P., et al. 2015, A&A, 575, A96
Guarneri, F., Calderone, G., Cristiani, S., et al. 2021, MNRAS, 506, 2471
Harris, C. R., Millman, K. J., van der Walt, S. J., et al. 2020, Nature, 585, 357
Henriques, B. M. B., White, S. D. M., Thomas, P. A., et al. 2015, MNRAS, 451, 2663
Hezaveh, Y. D., Perreault Levasseur, L., & Marshall, P. J. 2017, Nature, 548, 555
Hildebrandt, H., Arnouts, S., Capak, P., et al. 2010, A&A, 523, A31
Huertas-Company, M., Gravet, R., Cabrera-Vives, G., et al. 2015, ApJS, 221, 8
Ibata, R. A., McConnachie, A., Cuillandre, J.-C., et al. 2017, ApJ, 848, 128
Ilbert, O., McCracken, H. J., Le Fèvre, O., et al. 2013, A&A, 556, A55
Ivezic, Z., Axelrod, T., Brandt, W. N., et al. 2008, Serb. Astron. J., 176, 1
Kennicutt, R. C., & Evans, N. J. 2012, ARA&A, 50, 531

Kingma, D. P., & Ba, J. 2014, arXiv e-prints [arXiv:1412.6980]
Laureijs, R., Amiaux, J., Arduini, S., et al. 2011, arXiv e-prints [arXiv:1110.3193]
Leistedt, B., Alsing, J., Peiris, H., Mortlock, D., & Leja, J. 2023, ApJS, 264, 23
Li, R., Napolitano, N. R., Feng, H., et al. 2022a, A&A, 666, A85
Li, C., Zhang, Y., Cui, C., et al. 2022b, MNRAS, 509, 2289
López-López, X., Bolzonella, M., Pozzetti, L., et al. 2024, A&A, 691, A136
LSST Science Collaboration (Abell, P. A., et al.) 2009, arXiv e-prints [arXiv:0912.0201]
Maciaszek, T., Ealet, A., Jahnke, K., et al. 2016, SPIE Conf. Ser., 9904, 99040T
Merlin, E., Fontana, A., Castellano, M., et al. 2018, MNRAS, 473, 2098
Miyazaki, S., Komiyama, Y., Kawanomoto, S., et al. 2018, PASJ, 70, S1
Mucesh, S., Hartley, W. G., Palmese, A., et al. 2021, MNRAS, 502, 2770
Nair, V., & Hinton, G. E. 2010, ICML 2010, 807
Oke, J. B., & Gunn, J. E. 1983, ApJ, 266, 713
Pasquet, J., Bertin, E., Treyer, M., Arnouts, S., & Fouchez, D. 2019, A&A, 621, A26
Pedregosa, F., Varoquaux, G., Gramfort, A., et al. 2011, J. Mach. Learn. Res., 12, 2825
Peng, Y.-J., Lilly, S. J., Kovač, K., et al. 2010, ApJ, 721, 193
Pozzetti, L., Bolzonella, M., Zucca, E., et al. 2010, A&A, 523, A13
Prokhorenkova, L., Gusev, G., Vorobev, A., Dorogush, A. V., & Gulin, A. 2018, Adv. Neural Inf. Process. Syst., 31, 6638
Razim, O., Cavuoti, S., Brescia, M., et al. 2021, MNRAS, 507, 5034
Rodighiero, G., Renzini, A., Daddi, E., et al. 2014, MNRAS, 443, 19
Rodrigo, C., & Solano, E. 2020, XIV.0 Scientific Meeting (virtual) of the Spanish Astronomical Society, 182
Rodrigo, C., Solano, E., & Bayo, A. 2012, SVO Filter Profile Service Version 1.0, IVOA Working Draft
Salpeter, E. E. 1955, ApJ, 121, 161
Sawicki, M. 2012, PASP, 124, 1208
Schreiber, C., Elbaz, D., Pannella, M., et al. 2017, A&A, 602, A96
Scoville, N., Aussel, H., Brusa, M., et al. 2007, ApJS, 172, 1
Signor, T., Rodighiero, G., Bisigello, L., et al. 2024, A&A, 685, A127
Simet, M., Chartab, N., Lu, Y., & Mobasher, B. 2021, ApJ, 908, 47
Springel, V., White, S. D. M., Jenkins, A., et al. 2005, Nature, 435, 629
Surana, S., Wadadekar, Y., Bait, O., & Bhosale, H. 2020, MNRAS, 493, 4808
Tagliaferri, R., Longo, G., Andreon, S., et al. 2003, Lect. Notes Comput. Sci., 2859, 226
Tanaka, M., Coupon, J., Hsieh, B.-C., et al. 2018, PASJ, 70, S9
Thorp, S., Alsing, J., Peiris, H. V., et al. 2024, ApJ, accepted [arXiv:2406.19437]
Tuccillo, D., Huertas-Company, M., Decencière, E., et al. 2018, MNRAS, 475, 894
Ucci, G., Ferrara, A., Pallottini, A., & Gallerani, S. 2018, MNRAS, 477, 1484
Virtanen, P., Gommers, R., Oliphant, T. E., et al. 2020, Nat. Methods, 17, 261
Weaver, J. R., Kauffmann, O. B., Ilbert, O., et al. 2022, ApJS, 258, 11
Werner, M. W., Roellig, T. L., Low, F. J., et al. 2004, ApJS, 154, 1
Wes McKinney 2010, in Proceedings of the 9th Python in Science Conference, eds. S. van der Walt, & J. Millman, 56
Williams, R. J., Quadri, R. F., Franx, M., van Dokkum, P., & Labbé, I. 2009, ApJ, 691, 1879

[1] Dipartimento di Fisica e Astronomia "Augusto Righi" - Alma Mater Studiorum Università di Bologna, via Piero Gobetti 93/2, 40129 Bologna, Italy
[2] INAF-Osservatorio di Astrofisica e Scienza dello Spazio di Bologna, Via Piero Gobetti 93/3, 40129 Bologna, Italy
[3] Instituto de Astrofísica e Ciências do Espaço, Universidade do Porto, CAUP, Rua das Estrelas, PT4150-762 Porto, Portugal
[4] DTx – Digital Transformation CoLAB, Building 1, Azurém Campus, University of Minho, 4800-058 Guimarães, Portugal
[5] Faculdade de Ciências da Universidade do Porto, Rua do Campo de Alegre, 4150-007 Porto, Portugal
[6] Department of Astronomy, University of Geneva, ch. d'Ecogia 16, 1290 Versoix, Switzerland
[7] INAF, Istituto di Radioastronomia, Via Piero Gobetti 101, 40129 Bologna, Italy
[8] Dipartimento di Fisica e Astronomia "G. Galilei", Università di Padova, Via Marzolo 8, 35131 Padova, Italy
[9] INAF-Osservatorio Astronomico di Capodimonte, Via Moiariello 16, 80131 Napoli, Italy
[10] INFN section of Naples, Via Cinthia 6, 80126 Napoli, Italy
[11] INAF-Osservatorio Astronomico di Trieste, Via G. B. Tiepolo 11, 34143 Trieste, Italy
[12] Dipartimento di Fisica e Astronomia, Università di Firenze, via G. Sansone 1, 50019 Sesto Fiorentino, Firenze, Italy
[13] INAF-Osservatorio Astrofisico di Arcetri, Largo E. Fermi 5, 50125 Firenze, Italy
[14] INAF-Osservatorio Astronomico di Padova, Via dell'Osservatorio 5, 35122 Padova, Italy
[15] Instituto de Astrofísica de Canarias (IAC); Departamento de Astrofísica, Universidad de La Laguna (ULL), 38200 La Laguna, Tenerife, Spain
[16] Institute of Space Sciences (ICE, CSIC), Campus UAB, Carrer de Can Magrans, s/n, 08193 Barcelona, Spain
[17] Université Paris-Saclay, CNRS, Institut d'astrophysique spatiale, 91405 Orsay, France
[18] ESAC/ESA, Camino Bajo del Castillo, s/n., Urb. Villafranca del Castillo, 28692 Villanueva de la Cañada, Madrid, Spain
[19] School of Mathematics and Physics, University of Surrey, Guildford, Surrey GU2 7XH, UK
[20] INAF-Osservatorio Astronomico di Brera, Via Brera 28, 20122 Milano, Italy
[21] IFPU, Institute for Fundamental Physics of the Universe, via Beirut 2, 34151 Trieste, Italy
[22] INFN, Sezione di Trieste, Via Valerio 2, 34127 Trieste, TS, Italy
[23] SISSA, International School for Advanced Studies, Via Bonomea 265, 34136 Trieste, TS, Italy
[24] Dipartimento di Fisica e Astronomia, Università di Bologna, Via Gobetti 93/2, 40129 Bologna, Italy
[25] INFN-Sezione di Bologna, Viale Berti Pichat 6/2, 40127 Bologna, Italy
[26] Max Planck Institute for Extraterrestrial Physics, Giessenbachstr. 1, 85748 Garching, Germany
[27] Universitäts-Sternwarte München, Fakultät für Physik, Ludwig-Maximilians-Universität München, Scheinerstrasse 1, 81679 München, Germany
[28] INAF-Osservatorio Astrofisico di Torino, Via Osservatorio 20, 10025 Pino Torinese (TO), Italy
[29] Dipartimento di Fisica, Università di Genova, Via Dodecaneso 33, 16146 Genova, Italy
[30] INFN-Sezione di Genova, Via Dodecaneso 33, 16146 Genova, Italy
[31] Department of Physics "E. Pancini", University Federico II, Via Cinthia 6, 80126 Napoli, Italy
[32] Dipartimento di Fisica, Università degli Studi di Torino, Via P. Giuria 1, 10125 Torino, Italy
[33] INFN-Sezione di Torino, Via P. Giuria 1, 10125 Torino, Italy
[34] INAF-IASF Milano, Via Alfonso Corti 12, 20133 Milano, Italy
[35] Centro de Investigaciones Energéticas, Medioambientales y Tecnológicas (CIEMAT), Avenida Complutense 40, 28040 Madrid, Spain
[36] Port d'Informació Científica, Campus UAB, C. Albareda s/n, 08193 Bellaterra (Barcelona), Spain
[37] Institute for Theoretical Particle Physics and Cosmology (TTK), RWTH Aachen University, 52056 Aachen, Germany
[38] Institut d'Estudis Espacials de Catalunya (IEEC), Edifici RDIT, Campus UPC, 08860 Castelldefels, Barcelona, Spain
[39] INAF-Osservatorio Astronomico di Roma, Via Frascati 33, 00078 Monteporzio Catone, Italy
[40] Dipartimento di Fisica e Astronomia "Augusto Righi" - Alma Mater Studiorum Università di Bologna, Viale Berti Pichat 6/2, 40127 Bologna, Italy
[41] Instituto de Astrofísica de Canarias, Calle Vía Láctea s/n, 38204 San Cristóbal de La Laguna, Tenerife, Spain
[42] Institute for Astronomy, University of Edinburgh, Royal Observatory, Blackford Hill, Edinburgh EH9 3HJ, UK
[43] Jodrell Bank Centre for Astrophysics, Department of Physics and Astronomy, University of Manchester, Oxford Road, Manchester M13 9PL, UK
[44] European Space Agency/ESRIN, Largo Galileo Galilei 1, 00044 Frascati, Roma, Italy

[45] Université Claude Bernard Lyon 1, CNRS/IN2P3, IP2I Lyon, UMR 5822, Villeurbanne F-69100, France
[46] Institute of Physics, Laboratory of Astrophysics, Ecole Polytechnique Fédérale de Lausanne (EPFL), Observatoire de Sauverny, 1290 Versoix, Switzerland
[47] UCB Lyon 1, CNRS/IN2P3, IUF, IP2I Lyon, 4 rue Enrico Fermi, 69622 Villeurbanne, France
[48] Departamento de Física, Faculdade de Ciências, Universidade de Lisboa, Edifício C8, Campo Grande PT1749-016, Lisboa, Portugal
[49] Instituto de Astrofísica e Ciências do Espaço, Faculdade de Ciências, Universidade de Lisboa, Campo Grande 1749-016 Lisboa, Portugal
[50] INAF-Istituto di Astrofisica e Planetologia Spaziali, via del Fosso del Cavaliere, 100, 00100 Roma, Italy
[51] INFN-Padova, Via Marzolo 8, 35131 Padova, Italy
[52] Université Paris-Saclay, Université Paris Cité, CEA, CNRS, AIM, 91191 Gif-sur-Yvette, France
[53] Institut de Ciencies de l'Espai (IEEC-CSIC), Campus UAB, Carrer de Can Magrans, s/n Cerdanyola del Vallés, 08193 Barcelona, Spain
[54] School of Physics, HH Wills Physics Laboratory, University of Bristol, Tyndall Avenue, Bristol BS8 1TL, UK
[55] Istituto Nazionale di Fisica Nucleare, Sezione di Bologna, Via Irnerio 46, 40126 Bologna, Italy
[56] Institute of Theoretical Astrophysics, University of Oslo, P.O. Box 1029, Blindern 0315, Oslo, Norway
[57] Jet Propulsion Laboratory, California Institute of Technology, 4800 Oak Grove Drive, Pasadena, CA 91109, USA
[58] Department of Physics, Lancaster University, Lancaster LA1 4YB, UK
[59] Felix Hormuth Engineering, Goethestr. 17, 69181 Leimen, Germany
[60] Technical University of Denmark, Elektrovej 327, 2800 Kgs. Lyngby, Denmark
[61] Cosmic Dawn Center (DAWN), Copenhagen, Denmark
[62] Max-Planck-Institut für Astronomie, Königstuhl 17, 69117 Heidelberg, Germany
[63] Department of Physics and Astronomy, University College London, Gower Street, London WC1E 6BT, UK
[64] Department of Physics and Helsinki Institute of Physics, Gustaf Hällströmin katu 2, 00014 University of Helsinki, Helsinki, Finland
[65] Aix-Marseille Université, CNRS/IN2P3, CPPM, Marseille, France
[66] Université de Genève, Département de Physique Théorique and Centre for Astroparticle Physics, 24 quai Ernest-Ansermet, CH-1211 Genève 4, Switzerland
[67] Department of Physics, P.O. Box 64, 00014 University of Helsinki, Finland
[68] Helsinki Institute of Physics, Gustaf Hällströmin katu 2, University of Helsinki, Helsinki, Finland
[69] NOVA optical infrared instrumentation group at ASTRON, Oude Hoogeveensedijk 4, 7991PD Dwingeloo, The Netherlands
[70] Universität Bonn, Argelander-Institut für Astronomie, Auf dem Hügel 71, 53121 Bonn, Germany
[71] INFN-Sezione di Roma, Piazzale Aldo Moro, 2 - c/o Dipartimento di Fisica, Edificio G. Marconi 00185 Roma, Italy
[72] Aix-Marseille Université, CNRS, CNES, LAM, Marseille, France
[73] Department of Physics, Institute for Computational Cosmology, Durham University, South Road, Durham DH1 3LE, UK
[74] Institut d'Astrophysique de Paris, UMR 7095, CNRS, and Sorbonne Université, 98 bis boulevard Arago, 75014 Paris, France
[75] Université Paris Cité, CNRS, Astroparticule et Cosmologie, 75013 Paris, France
[76] University of Applied Sciences and Arts of Northwestern Switzerland, School of Engineering, 5210 Windisch, Switzerland
[77] Institut d'Astrophysique de Paris, 98bis Boulevard Arago, 75014 Paris, France
[78] Institut de Física d'Altes Energies (IFAE), The Barcelona Institute of Science and Technology, Campus UAB, 08193 Bellaterra (Barcelona), Spain
[79] European Space Agency/ESTEC, Keplerlaan 1, 2201 AZ Noordwijk, The Netherlands
[80] School of Mathematics, Statistics and Physics, Newcastle University, Herschel Building, Newcastle-upon-Tyne NE1 7RU, UK
[81] Department of Physics and Astronomy, University of Aarhus, Ny Munkegade 120, DK-8000 Aarhus C, Denmark
[82] Space Science Data Center, Italian Space Agency, via del Politecnico snc, 00133 Roma, Italy
[83] Centre National d'Etudes Spatiales – Centre spatial de Toulouse, 18 avenue Edouard Belin, 31401 Toulouse Cedex 9, France
[84] Institute of Space Science, Str. Atomistilor, nr. 409 Măgurele, Ilfov 077125, Romania
[85] Departamento de Astrofísica, Universidad de La Laguna, 38206 La Laguna, Tenerife, Spain
[86] Institut für Theoretische Physik, University of Heidelberg, Philosophenweg 16, 69120 Heidelberg, Germany
[87] Institut de Recherche en Astrophysique et Planétologie (IRAP), Université de Toulouse, CNRS, UPS, CNES, 14 Av. Edouard Belin, 31400 Toulouse, France
[88] Université St Joseph; Faculty of Sciences, Beirut, Lebanon
[89] Departamento de Física, FCFM, Universidad de Chile, Blanco Encalada 2008, Santiago, Chile
[90] Universität Innsbruck, Institut für Astro- und Teilchenphysik, Technikerstr. 25/8, 6020 Innsbruck, Austria
[91] Satlantis, University Science Park, Sede Bld 48940, Leioa-Bilbao, Spain
[92] Infrared Processing and Analysis Center, California Institute of Technology, Pasadena, CA 91125, USA
[93] Instituto de Astrofísica e Ciências do Espaço, Faculdade de Ciências, Universidade de Lisboa, Tapada da Ajuda, 1349-018 Lisboa, Portugal
[94] Universidad Politécnica de Cartagena, Departamento de Electrónica y Tecnología de Computadoras, Plaza del Hospital 1, 30202 Cartagena, Spain
[95] INFN-Bologna, Via Irnerio 46, 40126 Bologna, Italy
[96] Kapteyn Astronomical Institute, University of Groningen, PO Box 800, 9700 AV Groningen, The Netherlands
[97] Dipartimento di Fisica, Università degli studi di Genova, and INFN-Sezione di Genova, via Dodecaneso 33, 16146 Genova, Italy
[98] Astronomical Observatory of the Autonomous Region of the Aosta Valley (OAVdA), Loc. Lignan 39, I-11020 Nus (Aosta Valley), Italy
[99] Junia, EPA department, 41 Bd Vauban, 59800 Lille, France
[100] ICSC - Centro Nazionale di Ricerca in High Performance Computing, Big Data e Quantum Computing, Via Magnanelli 2, Bologna, Italy
[101] Instituto de Física Teórica UAM-CSIC, Campus de Cantoblanco, 28049 Madrid, Spain
[102] CERCA/ISO, Department of Physics, Case Western Reserve University, 10900 Euclid Avenue, Cleveland, OH 44106, USA
[103] Laboratoire Univers et Théorie, Observatoire de Paris, Université PSL, Université Paris Cité, CNRS, 92190 Meudon, France
[104] Dipartimento di Fisica e Scienze della Terra, Università degli Studi di Ferrara, Via Giuseppe Saragat 1, 44122 Ferrara, Italy
[105] Istituto Nazionale di Fisica Nucleare, Sezione di Ferrara, Via Giuseppe Saragat 1, 44122 Ferrara, Italy
[106] Dipartimento di Fisica "Aldo Pontremoli", Università degli Studi di Milano, Via Celoria 16, 20133 Milano, Italy
[107] Université de Strasbourg, CNRS, Observatoire astronomique de Strasbourg, UMR 7550, 67000 Strasbourg, France
[108] Kavli Institute for the Physics and Mathematics of the Universe (WPI), University of Tokyo, Kashiwa, Chiba 277-8583, Japan
[109] Dipartimento di Fisica - Sezione di Astronomia, Università di Trieste, Via Tiepolo 11, 34131 Trieste, Italy
[110] Minnesota Institute for Astrophysics, University of Minnesota, 116 Church St SE, Minneapolis, MN 55455, USA
[111] Institute Lorentz, Leiden University, Niels Bohrweg 2, 2333 CA Leiden, The Netherlands
[112] Université Côte d'Azur, Observatoire de la Côte d'Azur, CNRS, Laboratoire Lagrange, Bd de l'Observatoire, CS 34229, 06304 Nice cedex 4, France

[113] Institute for Astronomy, University of Hawaii, 2680 Woodlawn Drive, Honolulu, HI 96822, USA
[114] Department of Physics & Astronomy, University of California Irvine, Irvine, CA 92697, USA
[115] Department of Astronomy & Physics and Institute for Computational Astrophysics, Saint Mary's University, 923 Robie Street, Halifax, Nova Scotia B3H 3C3, Canada
[116] Departamento Física Aplicada, Universidad Politécnica de Cartagena, Campus Muralla del Mar, 30202 Cartagena, Murcia, Spain
[117] Department of Physics, Oxford University, Keble Road, Oxford OX1 3RH, UK
[118] CEA Saclay, DFR/IRFU, Service d'Astrophysique, Bat. 709, 91191 Gif-sur-Yvette, France
[119] Institute of Cosmology and Gravitation, University of Portsmouth, Portsmouth PO1 3FX, UK
[120] Department of Computer Science, Aalto University, PO Box 15400, Espoo FI-00 076, Finland
[121] Caltech/IPAC, 1200 E. California Blvd., Pasadena, CA 91125, USA
[122] Ruhr University Bochum, Faculty of Physics and Astronomy, Astronomical Institute (AIRUB), German Centre for Cosmological Lensing (GCCL), 44780 Bochum, Germany
[123] DARK, Niels Bohr Institute, University of Copenhagen, Jagtvej 155, 2200 Copenhagen, Denmark
[124] Univ. Grenoble Alpes, CNRS, Grenoble INP, LPSC-IN2P3, 53, Avenue des Martyrs, 38000 Grenoble, France
[125] Department of Physics and Astronomy, Vesilinnantie 5, 20014 University of Turku, Turku, Finland
[126] Serco for European Space Agency (ESA), Camino bajo del Castillo, s/n, Urbanizacion Villafranca del Castillo, Villanueva de la Cañada 28692, Madrid, Spain
[127] ARC Centre of Excellence for Dark Matter Particle Physics, Melbourne, Australia
[128] Centre for Astrophysics & Supercomputing, Swinburne University of Technology, Hawthorn, Victoria 3122, Australia
[129] Department of Physics and Astronomy, University of the Western Cape, Bellville, Cape Town 7535, South Africa
[130] School of Physics and Astronomy, Queen Mary University of London, Mile End Road, London E1 4NS, UK
[131] ICTP South American Institute for Fundamental Research, Instituto de Física Teórica, Universidade Estadual Paulista, São Paulo, Brazil
[132] Oskar Klein Centre for Cosmoparticle Physics, Department of Physics, Stockholm University, Stockholm SE-106 91, Sweden
[133] Astrophysics Group, Blackett Laboratory, Imperial College London, London SW7 2AZ, UK
[134] Dipartimento di Fisica, Sapienza Università di Roma, Piazzale Aldo Moro 2, 00185 Roma, Italy
[135] Centro de Astrofísica da Universidade do Porto, Rua das Estrelas, 4150-762 Porto, Portugal
[136] Institute of Astronomy, University of Cambridge, Madingley Road, Cambridge CB3 0HA, UK
[137] Department of Astrophysics, University of Zurich, Winterthurerstrasse 190, 8057 Zurich, Switzerland
[138] Theoretical astrophysics, Department of Physics and Astronomy, Uppsala University, Box 515, 751 20 Uppsala, Sweden
[139] Department of Physics, Royal Holloway, University of London, London TW20 0EX, UK
[140] Mullard Space Science Laboratory, University College London, Holmbury St Mary, Dorking, Surrey RH5 6NT, UK
[141] Department of Physics and Astronomy, University of California, Davis, CA 95616, USA
[142] Department of Astrophysical Sciences, Peyton Hall, Princeton University, Princeton, NJ 08544, USA
[143] Niels Bohr Institute, University of Copenhagen, Jagtvej 128, 2200 Copenhagen, Denmark
[144] Center for Cosmology and Particle Physics, Department of Physics, New York University, New York, NY 10003, USA
[145] Center for Computational Astrophysics, Flatiron Institute, 162 5th Avenue, 10010 New York, NY, USA

Appendix A: Feature importances

In this appendix, we present the feature importance for models evaluated with CSMR. In standard ML terminology, feature importance refers to the quantification of the impact each feature has on the model's predictions. This is measured by considering the number of times a feature is used for splits across all trees in the ensemble and the corresponding improvement in the model's performance. The higher the number of times a feature is used and the greater the improvement, the more important the feature is considered, giving insights into the relative significance of different features in the data, for example, if and what certain filter or color is more important in correctly assessing a galaxy redshift, stellar mass, or star formation rate.

These findings are reported in Fig. A.1, where we show the feature importance for four different models, each one specifically trained to recover a single label, whether is $z_{\rm phot}$, $\log_{10}(M_\star/M_\odot)$, or $\log_{10}({\rm SFR}/M_\odot\,{\rm yr}^{-1})$, and a model trained on a set of pooled labels. In each case, to remove altogether every source of noise skewing the results, we are performing the training on the unperturbed catalog (see Sect. 4.3 for further details).

As expected, considering that most of the training galaxies are at $0 < z < 1.5$, the $H_{\rm E}$ band is by far the most important one in determining a galaxy's stellar mass (more than half importance); similarly, for photometric redshifts, the colors hold the most importance, more than single filter observations. Things are more mixed for star formation rates, as with the exception of $H_{\rm E}$ ($\sim$ 25%), all the other features hold similar importance (between 3% and 6%). When considering all the labels together, we observe a mix between the previous results, with $H_{\rm E}$ being still the most considered feature at $\sim$ 25% importance, followed by the colors.

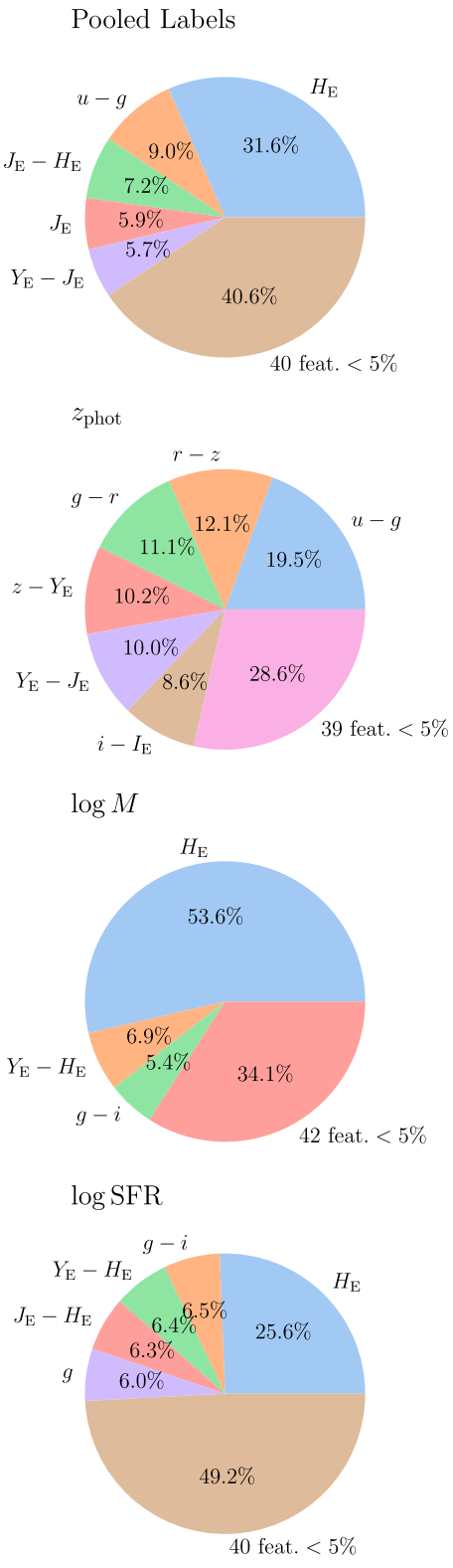

Fig. A.1. Pie chart highlighting the most important features in recovering the pooled labels with CSMR. The feature importance weights (in percentage) how much a single feature influences the final prediction. In the Pooled Labels and log_{10} SFR only cases, 45 features enter the model (magnitudes and all possible color permutations), only five have an importance over 5%.

Appendix B: Phosphoros results for the calibration fields

In Sect. 4.2, we reported the template-fitting results with Phosphoros to the EWS and EDF. In Fig. B.1, we report the corresponding Phosphoros run to the auxiliary fields at 16 and 25 ROS each. As expected, the performance is intermediate between the EDF and the EWS, though closer to the former. Anyway, it should always be kept in mind that the deeper the observations, the more distant and/or less massive galaxies will enter the catalogs, whose photometric redshifts and physical parameters are harder to properly assess, therefore reducing the expected metrics improvement.

Appendix C: Results with the paired labels approach

In Tabs. C.1–C.2, we report the results for the EWS with the paired labels approach. As described in Sect. 4.4, with this approach, we train each model with a set of features and labels obtained from the Phosphoros run to the corresponding depth (e.g., C16 features, labels from Phosphoros run to the C16 photometry), and test on Wide features and ground truth values obtained from the simulation.